V. I. Emel'yanov, A. E. Tarkhov, Two-stage mechanism of formation of ordered surface nanostructures under atomic deposition,
Comp. nanotechnol., 2015, Issue 4, 37–50

3. МОДЕЛЬНО-ОРИЕНТИРОВАННОЕ ПРОЕКТИРОВАНИЕ

3.1. ДВУХСТАДИЙНЫЙ МЕХАНИЗМ ОБРАЗОВАНИЯ ПОВЕРХНОСТНЫХ НАНОСТРУКТУР ПРИ ОСАЖДЕНИИ АТОМОВ

Емельянов Владимир Ильич, доктор физико-математических наук, профессор Физического факультета МГУ им. М. В. Ломоносова. E-mail: emel@em.msk.ru

Тархов Андрей Евгеньевич, студент Физического факультета МГУ им. М. В. Ломоносова

Аннотация: Развит двухстадийный механизм образования упорядоченных поверхностных наноструктур при осаждении атомов. На первой стадии, происходит кооперативная дефектно-деформационная (ДД) нуклеация затравочной наноструктуры, описываемая оригинальным детерминированным ДД уравнением типа уравнения Курамото-Сивашинского(КС) для концентрации мобильных адатомов (поверхностных дефектов). Поверхностный рельеф, образованный на стадии нуклеации, связанный с деформационным потенциалом поверхностного дефекта, служит самоорганизованной маской для последующего роста наноструктр, описываемого обычным уравнением Кардара-Паризи-Жанга-(КПЖ) для высоты рельефа. Компьютерные решения нелинейных ДДКС и КПЖ уравнений описывают двухстадийное образование, в зависимости от знака потенциала деформации поверхностного дефекта, неупорядоченных и гексагонально упорядоченных ансамблей наночастиц или сотовых наноструктур пор. Показано, что взаимодействие пространственных ДД гармоник на стадии кооперативной нуклеации играет ключевую роль в определении характеристик наноструктур

Ключевые слова: осаждение атомов, образование гексагонально упорядоченных ансамблей наночастиц и сотовых наноструктур пор, компьютерное моделирование

TWO-STAGE MECHANISM OF FORMATION OF ORDERED SURFACE NANOSTRUCTURES UNDER ATOMIC DEPOSITION

Emel'yanov Vladimir Il'ich, doctor of physico-mathematical Sciences, Professor. Physics Faculty, Lomonosov Moscow State University. E-mail: emel@em.msk.ru

Tarkhov Andrey Evgenyevich, student. Physics Faculty, Lomonosov Moscow State University

Abstract: Two-stage mechanism of formation of ordered surface nanostructures under atomic deposition is developed. At the first stage, the cooperative defect-deformational (DD) nucleation of seeding nanostructure occurs, described by the original deterministic DD Kuramoto-Sivashinsky (DDKS) equation for the concentration of mobile adatoms (surface defects). Periodic surface relief, formed at the nucleation stage, related to the surface defect deformation potential, serves as a self-organized mask for subsequent growth of nanostructures, described by the convential deterministic Kardar-Parisi-Zhang (KPZ) equation for the relief height. Computer simulations of nonlinear DDKS and KPZ equations describe the two-stage formation, in dependence on the sign of the surface defect deformation potential, of disordered and hexagonally ordered ensembles of nanoparticles or honeycomb void nanostructures. The spatial DD harmonics interaction during cooperative nucleation is shown to play the key role in determination of the resulting nanostructures characteristics

Index terms: atomic deposition, hexagonally ordered ensembles of nanoparticles and honeycomb void nanostructures formation, computer modeling

1. Introduction

In recent years, the spontaneous formation of periodic nanostructures upon the action of energy or particles fluxes on the surface of solids has become the subject of intensive studies [1]. One of main tools for the theoretical investigation of this phenomenon is the nonlinear Kuramoto-Sivashinsky (KS) equation [2,3]. Two-dimensional KS equations with specific variables are used for the description of nanostructuring of solid surfaces using ion beams [4] or electrochemical etching [5]. Authors of [6] derived anisotropic Kuramoto–Sivashinsky type for the surface corrugation h under laser ablation and used its solutions for description of surface periodic

ripple formation. A two-dimensional DDKS equation was derived for defect concentration in the defect-enriched surface solid layer, formed by laser irradiation [7], and its numerical solutions have been used for the interpretation of the formation of surface nano- and microstructures under the action of laser pulses [8].

In the works [9-11] the conception of the DDKS equation was extended to the ensemble of interacting with each other adatoms. First, in works [9,10], the theory of the surface defect-deformational (DD) instability in the system of mobile adatoms (surface defects), interacting via quasi-static surface acoustic (Rayleigh) waves has been developed. The mechanism of the surface DD instability consists in the following.

An initial surface fluctuation strain gives rise to strain-induced surface defect fluxes. This leads to the formation of the spatially nonuniform field of adatom concentration, which via the deformation potential of adatoms and also via the local renormalization of the surface energy, nonuniformly deforms the surface and the underlying elastic continuum, increasing thus the initial strain. In doing so, the deformation of the elastic continuum is described by quasi-Rayleigh static elastic displacements. At exceeding of a certain critical value of the adatom concentration, such positive feedback leads to the onset of DD instability with arising of nanometer scale surface strain and relief modulations and piling of adatoms at extrema of the surface strain.

Then, in the work [11] it was shown that, under some restrictions, starting equations of the surface DD self-organization [9,10] can be reduced to a closed two-dimensional, nonlinear partial differential equation for adatom concentration of the KS equation type. In the mean field approximation (MFA), the obtained DDKS equation is reduced to the surface DDKS equation with the critical behavior. It describes the threshold self-organization of DD surface adatom nanostructures that can serve as a seed for the subsequent growth of nanostructures in the processes of surface nanostructuring, which involve the generation of mobile surface defects (adatoms, dimers and other species).

In this work, we numerically investigate the nucleation stage described by the DDKS equation for surface defect concentration [11], focusing on the role of the negative sign of the quadratic nonlinearity occurring in it. Besides, we consider for the first time the second (growth) stage of surface nanostructures formation.

It is shown that, due to the negative sign of the quadratic nonlinear term in the DDKS equation, the final field of surface defect concentration after the first (cooperative DD nucleation) stage corresponds to hexagonally ordered honeycomb structure of voids.

The cooperative nucleation is terminated by the higher-order cubic DD nonlinearity due to renormalization of the defect diffusivity by the strain [10] and is replaced by the growth stage. The latter is described here by the conventional two-dimensional nonlinear Kardar-Parisi-Zhang (KPZ) equation for the surface relief height h [12]. As the initial condition in numerical solution of the KPZ equation, we use the surface relief formed after the termination of the nucleation stage which is coupled by the surface defect deformation potential with the nucleated honeycomb defect concentration structure.

It is shown that the sign of the surface defect deformation potential plays a crucial role in determination of the type of final nanostructure of surface relief formed in this two-stage process. In the case of positive surface defect deformation potential, the honeycomb void nanostructure of surface relief is formed, while in the case of negative defect deformation potential, a hexagonal ensemble of nanoparticles is formed similar to [11]. The periodicity of final surface structures is determined by that of the seeding surface defect concentration field, i.e. is determined at the first, cooperative DD nucleation stage. In this respect, results of the present paper corroborate results of the work [11] where only the nucleation stage was

considered predicting formation of nanoparticle ensemble.

The key role of nonlinear interactions of DD harmonics at the cooperative nucleation stage in shaping the symmetry of the final nanostructures, revealed in [11], is also preserved in the two-stage process. We demonstrate this by considering dynamics of Fourier-spectra in case of hexagonal nanoparticles and void nanostructures formation and by comparing images of nucleated and final surface structures. We reveal the importance of second harmonic and sum-frequency generation processes for the existence of stationary solutions of DDKS equation, and we demonstrate the formation of a bimodal (with two sizes of nanoparticles) ensemble due to the nonlinear effects of parametric degenerate DD decay and sum-frequency generation. We put forward an idea for purification of supercrystalline structures obtained by atomic deposition and show results of computer simulation corroborating it.

In Sec.4 we briefly discuss the relevance of the developed theory to experimental data. We compare the results obtained by computer simulations with experimental data for void structure and nanoparticle ensemble formation and show the similarity of surface relief morphology predicted by simulation and experimental one.

1. Cooperative DD nucleation of ordered surface defect concentration nanostructures

1.1. Defect-Deformational Kuramoto-Sivashinsky equation for adatom concentration

In Sec.1.1 and 1.2, for completeness of exposition, we outline the DD approach developed in [9,10].

Let us consider the surface $z = 0$ of a solid (*z*-axis directed into the medium) with mobile adatoms (defects). The elastic force acting on a defect,

$$\mathbf{F}(\mathbf{r}) = \theta_d \operatorname{grad}\left(\xi + l_d^2 \Delta\xi\right), \qquad (1)$$

where $\mathbf{r} = (x, y)$, $\Delta = \partial^2/\partial x^2 + \partial^2/\partial y^2$, $\operatorname{grad} = \mathbf{e}_\mathbf{x}(\partial/\partial x) + \mathbf{e}_\mathbf{y}(\partial/\partial y)$, $\mathbf{e}_\mathbf{x}$ and $\mathbf{e}_\mathbf{y}$ are unit vectors along the *x* and *y* axes, respectively, $\xi = \xi(x, y)$ is the surface strain, l_d is the characteristic length of the defect-atom interaction lying in nanometer diapason (see [9]). The deformation potential of the surface defect θ_d, can have different signs depending on the nature of surface defect. It will be shown below that the sign of the deformation potential of surface defect plays a crucial role in determination of the type of surface nanostructure formed in the two-stage formation process.

The surface defect flux consists of the diffusion and strain-induced parts:

$$\mathbf{j}_d = -D_d \operatorname{grad} N_d + \frac{D_d}{k_B T}\theta_d N_d \operatorname{grad}\left(\xi + l_d^2 \Delta\xi\right), \qquad (2)$$

where D_d is the coefficient of the surface diffusion, k_B is the Boltzman constant, T is the temperature, $N_d\,(\mathrm{cm}^{-2})$ is the concentration of surface defects (adatoms or adatom dimers).

From the continuity equation, with allowance for $\mathbf{j}_d$ and neglecting the renormalization of the defect diffusivity by the strain, we obtain the equation for N_d. To close this equation, we need to express the surface strain ξ through the concentration of the surface defects N_d. This has been done in Refs. [9,10] with the help of solution of the equation for the displacement vector $\mathbf{u} = \mathbf{u}(\mathbf{r}, z)$ in an isotropic semi-infinite medium with boundary conditions involving the surface defect concentration.

In the MFA, the surface concentration of defects is represented as $N_d(\mathbf{r}, t) = N_{d0} + N_{d1}(\mathbf{r}, t)$, where N_{d0} is the spatially uniform concentration and $N_{d1}(\mathbf{r}, t)$ is the spatially non-uniform component that spontaneously arises above the DD instability threshold. Under the condition $|N_{d1}(\mathbf{r}, t)| < N_{d0}$, the DDKS equation derived in [11] has the form

$$\frac{\partial N_{d1}}{\partial t} = -\frac{1}{\tau}N_{d1} - D_d(\varepsilon - 1)\Delta N_{d1} - D_d \varepsilon l_d^2 \Delta^2 N_{d1} - \frac{D_d}{N_{dc}}(\nabla N_{d1})^2, \qquad (3)$$

where τ is the surface defect lifetime, the control parameter $\varepsilon = N_{d0}/N_{dc}$, where the critical surface defect concentration

$$N_{dc} = \rho c_l^2 (1 - \beta) k_B T a / {\theta_d}^2, \qquad (4)$$

a is the crystal lattice parameter, ρ is the medium density, $\beta = c_t^2/c_l^2$, c_l and c_t are the longitudinal and transverse sound velocities, respectively. In derivation of Eq.(3), only the normal defect-induced stress component was taken into account in boundary conditions for medium displacement vector $\mathbf{u}$ at the surface z=0 and the lateral components occurring due to the renormalization of the surface energy by surface defects were neglected.

The spatially uniform defect concentration N_{d0} is found as a steady state solution of the spatially uniform equation for adatom concentration $N_{d0} = \tau G_d$, where G_d is the rate of adatom generation. The parameter N_{d0} (i.e., ε) plays the role of a control parameter of the surface DD instability. Thus, it is supposed that surface defects have two states: the source reservoir state with concentration N_{d0} and the self-organized state with concentration N_{d1}. We assume that the source of defects is inexhaustible and stationary, so $N_{d0} = \text{const}$.

1.2. The dimensionless DDKS equation and its linear analysis

Let us introduce dimensionless coordinates: $X = x/l_d$, $Y = y/l_d$, the dimensionless time $T = tD_d/l_d^2$, the dimensionless relaxation constant $\Gamma = l_d^2/\tau D_d$ and the dimensionless nonuniform defect concentration $n = N_{d1}/N_{dc}$. Then, from Eq.(3), we obtain the following dimensionless DDKS equation:

$$\frac{\partial n}{\partial T} = -\Gamma n - (\varepsilon - 1)\Delta n - \varepsilon\Delta^2 n - (\nabla n)^2, \qquad (5)$$

where $\Delta = \partial^2/\partial X^2 + \partial^2/\partial Y^2$ and $\nabla = \mathbf{e}_x \partial/\partial X + \mathbf{e}_y \partial/\partial Y$. The equation (5) is the two-dimensional nonlinear partial differential equation with the first-order time derivative and the fourth-order spatial derivatives.

The linear analysis of Eq. (5) determines the region of dimensionless parameters Γ and ε, in which the initial perturbation exponentially increases with time (region of instability in the phase plane Γ, ε).

The linear solution of Eq.(5) represents a grating of the surface defect concentration

$$n(\mathbf{R},T) = n(\mathbf{Q},t)\exp(i\mathbf{QR}) = A\exp\left[\lambda(Q)T + i\mathbf{QR}\right] \qquad (6)$$

Hereinafter, $\mathbf{R} = \{X, Y\}$, $\mathbf{Q} = \{q_x l_d, q_y l_d\}$, q_x, q_y are wavevectors in the real dimensional space, and $A = \text{const}$ (initial white noise).

The surface defect concentration grating (6) is coupled with the surface strain grating

$$\xi(\mathbf{R},t) = (\text{div}\,\mathbf{u})_{z=0} = \sum_{\mathbf{Q}} \xi(\mathbf{Q},t)\exp(i\mathbf{QR}), \qquad (7)$$

where $\xi(\mathbf{Q},t) = \eta_d N_d(\mathbf{Q},t)$, and the DD coupling coefficient $\eta_d = \theta_d / a\rho c_l^2(1-\beta)$ [9]. Each pair of Fourier-components $n(\mathbf{Q},t)$, Eq.(6), and $\xi(\mathbf{Q},t)$, Eq.(7), describes the surface DD grating with the wave vector $\mathbf{Q}$. Besides, the surface defect concentration field is coupled with surface relief field (see Eq. (12)).

For the growth rate, we obtain

$$\lambda(Q) = (\varepsilon - 1)Q^2 - \varepsilon Q^4 - \Gamma \qquad (8)$$

The maximum growth rate λ_m is reached at $Q = Q_m = \left((\varepsilon - 1)/2\varepsilon\right)^{1/2}$. The period of the dominant DD harmonic $\Lambda_m = 2\pi/Q_m$ determines the characteristic dimensionless scale of the DD structure. The growth rate of this dominant DD harmonic (the characteristic inverse time of nanostructure formation) is

$$\lambda(Q_m) = \lambda_m = \left(\frac{(\varepsilon - 1)^2}{4\varepsilon}\right) - \Gamma \qquad (9)$$

In dimensional form the period of the DD structure, as a function of N_{d0}, at T=const, has the form

$$\Lambda_m(N_{d0}) = \sqrt{8\pi}\, l_d \left(1 - \frac{N_{dc}}{N_{d0}}\right)^{-1/2}, \qquad (10)$$

where the critical defect concentration is given by Eq.(4). At the control parameter $N_{d0} \to N_{dc}$ ($N_{d0} > N_{dc}$), the period $\Lambda_m(N_{d0}) \to \infty$. At $N_{d0} < N_{dc}$, the DD instability and corresponding surface nanostructuring do not occur.

If $N_{d0} = \text{const}$, then the period is the function of the temperature

$$\Lambda_m(T) = \sqrt{8\pi}\, l_d \left(1 - \frac{T}{T_c}\right)^{-1/2}, \qquad (11)$$

where the critical temperature $T_c = \theta_d^{\,2} N_{d0} / a\rho c_l^2 (1-\beta) k_B$. At $T \to T_c$ from below, $\Lambda_m(T) \to \infty$. At $T > T_c$, the DD instability and corresponding surface nanostructuring does not occur.

In the instability region, where the growth rate $\lambda(Q)$ is positive, the initial (linear) stage is characterized by the exponential growth of the amplitude of the DD gratings with time from an initial (fluctuation) level. The condition $\lambda(Q) = 0$ determines the boundary of the region of the DD surface instability in *Q*-space (the fundamental DD harmonics excitation band). Fig. 1 shows two unstable bands obtained at one and the same value of the control parameter Γ = 0.158 and two different values of the second control parameter: ε = 2.18 and ε = 2.4.

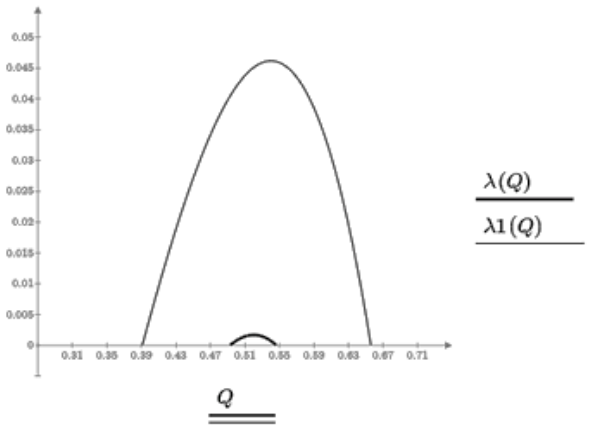

Fig. 1. The dependence of the dimensionless growth rate $\lambda(Q)$ of the DD grating on the dimensionless wavevector *Q*. Obtained with the help of Eq.(8) at Γ = 0.158 and two values of control parameter: ε = 2.18 (the lower curve $\lambda_1(Q)$) and ε = 2.4 (the upper curve $\lambda(Q)$)

It is seen that the very narrow band of DD harmonics is excited just above the DD instability threshold (*Γ* = 0.158, *ε* = 2.18) with small growth rate $\lambda_1(Q)$. It will be shown in Sec.2 that in this case, the cooperative DD nucleation, described by the DDKS equation (5), leads to the formation of hexagonally ordered (honeycomb) seeding ensemble of voids, which depends essentially on nonlinear effects such as second harmonic and sum-frequency generation (Sec.5). On the contrary, well above the DD instability threshold (*Γ* = 0.158, *ε* = 2.4, the curve $\lambda(Q)$), at first, a disordered, rough seeding void ensemble is formed (Sec.3), and then, in highly nonlinear regime, degenerate parametric DD decay and sum-frequency generation take place and a bimodal quasi-ordered nanoparticle ensemble is formed (Sec.6).

2. Computer simulations of the DDKS equation just above threshold. Formation of honeycomb seeding void structure of surface defect concentration at the nucleation stage

In computer simulations of the dimensionless DDKS equation (5), we use the two-stage Rosenbrock scheme with complex coefficients for stiff systems with L3-stability and precision $O(\tau^4)$ in time and $O(h^4)$ in space[13,14]. We use periodic boundary conditions for the square grid: $(x + L, y, t) = n(x, y, t)$, $n(x, y + L, t) = n(x, y, t)$, where L is the size of a region under consideration. The initial surface defect concentration $n(x, y, t = 0)$ is random with a uniform distribution on the interval.

We set in Eq.(5) the control parameters values *Γ* = 0.158 and *ε* = 2.18, corresponding to the narrow excitation band (Fig.1, the lower curve $\lambda_1(Q)$). Fig. 2 shows 2D images of surface defect concentration field obtained by simulation of Eq.(5) at different times. It is seen that the gradual ordering of surface defects occurs with time leading to the formation of final honeycomb void structure.

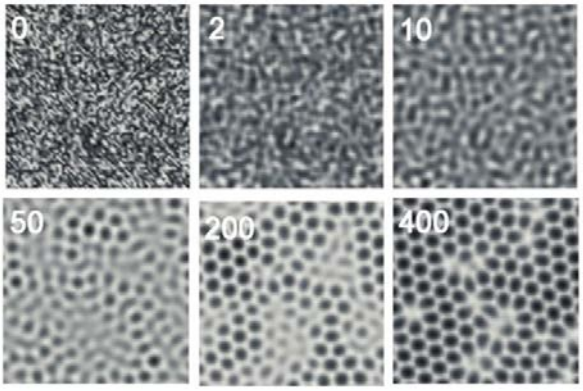

Fig. 2. 2D images of surface defect concentration field obtained by simulation of the DDKS equation (5) with *ε* = 2.18, *Γ* = 0.158 at different nucleation times *T* = 0, 2, 10, 50, 200 и 400 (black color corresponds to surface defect concentration minima, white color corresponds to concentration maxima)

The sequence of corresponding 3D images, shown in Fig. 2, elucidates the dynamics of formation of the final honeycomb structure of surface defect concentration field (nucleation time *T*=400). The formation of such hexagonally ordered ensemble of concentration depressions is due to the negative sign of the quadratic nonlinearity in Eq.(5). In contrast, it can be shown that the positive quadratic nonlinearity sign leads to the formation of hexagonal grid of mounds.

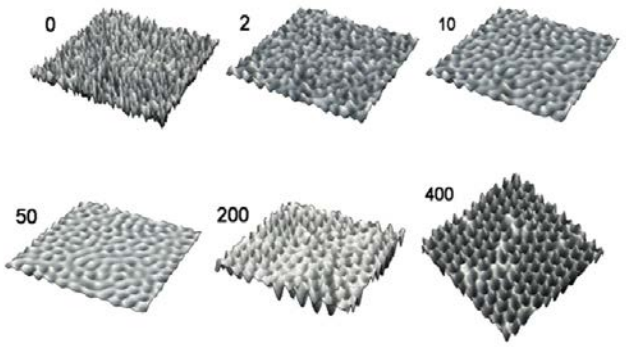

Fig. 3. 3D images of surface defect concentration field obtained by simulation of the DDKS equation (5). Values of equation parameters are the same as in Fig.2. Numbers designate corresponding nucleation times *T* = 0, 2, 10, 50, 200 и 400

Corresponding images of 3D Fourier spectrum, shown in Fig.4, give the additive information about the dynamics of honeycomb void structure formation. It is seen that on the linear stage of the DD instability, from initial spatially white noise (*T*=0), the ring of finite thickness is formed (*T*=10, 50). This ring corresponds to lamellar-like structure which is universal on small times of the DD surface self-organization [8,11]. The angular selection of the wavevectors of the DD harmonics (nucleation times *T*=50, 200, 400) at the nonlinear stage of the DD instability eventually leads to formation of honeycomb void structure (*T*=400).

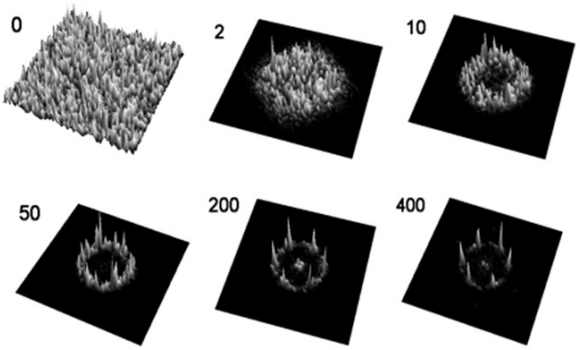

Fig.4. Computer images of 3D Fourier-spectrum corresponding to images of the surface defect concentration field at nucleation times *T*=0, 2, 10, 50, 200 and 500, shown in Fig.2 and Fig.3

Depending on the values of control parameters ε and Γ in the DDKS equation (5), different evolution routes of the surface defect concentration field are possible leading to the formation of a variety of final defect concentration structures. In addition to the ordered hexagonal structure of the defect concentration, in Sec.3 and Sec.6, we investigate two examples of formation of the rough surface nanorelief structure and the bimodal nanoparticle ensemble.

2. Growth of hexagonal nanoparticle and honeycomb void ensembles

2.1. Dimensionless KPZ growth equation

Due to the surface defect deformation potential, the final honeycomb structure of surface defect concentration (Fig. 3, nucleation time *T*=400) formed at nucleation stage is coupled with corresponding surface relief. The formula for the defect-surface relief coupling follows from the solution of the surface defect quasi-Rayleigh wave problem [9,10]. Using formulas for components of the displacement vector in the defect-induced quasi-Rayleigh (quasi-static) wave from [9], we obtain

$$h(\mathbf{R},t)=\theta_d\sum_{\mathbf{Q}}\left(n(\mathbf{Q},t)/Q\right)\exp\left(i\mathbf{QR}\right), \qquad (12)$$

where $h(\mathbf{R},t)$ is the height of the surface relief and θ_d is the surface defect deformation potential occurring in Eq. (1) which can have positive as well as negative signs depending on the type of surface defect and peculiarities of surface defect-strain interaction.

We assume that the time moment *t*=0 in Eq.(12) corresponds to the DD nonlinearity-related termination of the nucleation stage (see the discussion of this point in [10]) and use $h(\mathbf{R},0)$ from Eq. (12) as the initial condition in the conventional KPZ equation [12] for $h(\mathbf{R},t)$:

$$\frac{\partial h}{\partial t}=D_d\Delta h+\frac{v_n}{2}\left(\nabla h\right)^2, \qquad (13)$$

where v_n is the rate of growth along the normal to the surface which is assumed to be known. Introducing the dimensionless surface relief height $h=H/l_d$, the dimensionless time $T=tv_n/2l_d$ and the control parameter

$\delta = 2D_d/v_n l_d$, we obtain from Eq.(13) the dimensionless KPZ equation

$$\frac{\partial H}{\partial T} = \delta \Delta H + (\nabla H)^2 \qquad (14)$$

2.2. Growth of nanoparticle ensemble in the case of negative surface defect deformation potential

First, we consider the case of negative surface defect deformation potential $\gamma_d < 0$ in Eq.(12). In this case, the initial surface relief (the initial condition for the growth KPZ equation (14) at $T = T_{growth} = 0$) corresponds to the seeding nanoparticle ensemble (Fig.5) that leads to growth of final nanoparticle ensemble.

Fig. 5 shows the final honeycomb void structure of surface defect concentration formed at the cooperative nucleation stage at $T = 400$, the corresponding initial surface relief structure at $T_{growth} = 0$ (the initial condition for the KPZ growth equation (14)) and the final nanoparticle ensemble formed at $T_{growth} = 20$ in the two-stage cooperative nucleation-growth process.

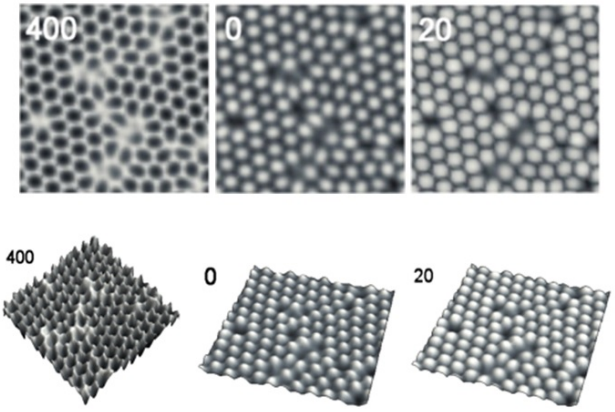

Fig. 5. (Top, from left to right) 2D images: of the surface defects concentration structure formed at the cooperative nucleation stage at nucleation time $T = 400$, the initial relief structure at the growth time Tgrowth=0, and the final relief structure obtained as the solution of the KPZ growth Eq. (14) with $\delta = 10^{-2}$ at Tgrowth=20 (black color corresponds to surface defect concentration minima and surface relief maxima, white color corresponds to concentration maxima and surface relief minima); (bottom) corresponding 3D images

Fig.6 shows the cross section of the surface relief after more prolong growth ($T_{growth} = 40$).

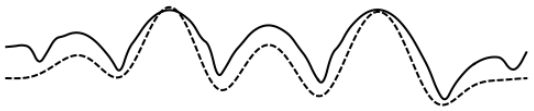

Fig. 6. (Dashed curve) cross section of 3D image of initial surface relief obtained at the cooperative nucleation stage; (full curve) surface relief obtained by computer simulation of the KPZ equation (14) with $\delta = 10^{-2}$ at $T_{growth} = 40$

It is seen that the growth does not affect essentially the size of nanoparticles but makes them to be more closely packed changing their shape to mound-like one.

2.3. Growth of honeycomb void structure of surface relief in the case of positive surface defect deformation potential

Now, let us consider the case of positive sign of the surface defect deformation potential $\gamma_d > 0$ occurring in Eq. (12). In this case, the initial surface relief (the initial condition for the growth KPZ equation (14) at $T = T_{growth} = 0$) is the seeding honeycomb void ensemble (Fig.5, the growth time T=0) that leads to growth of final honeycomb void ensemble.

Fig. 7 shows the final honeycomb structure of surface defect concentration formed at the cooperative nucleation stage (nucleation time T = 2000), corresponding initial surface relief structure (the initial condition for the growth equation (14), T_{growth}=0) and the final honeycomb void ensemble formed in the two-stage cooperative nucleation-growth process (T_{growth}=30).

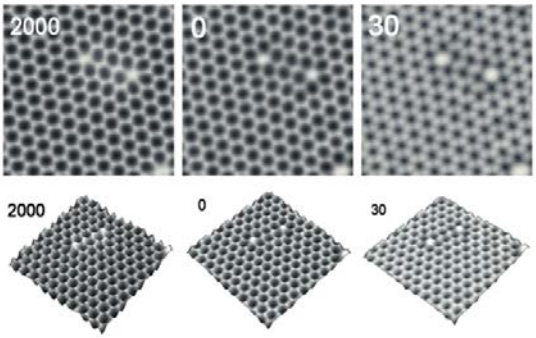

Fig. 7. (Top, from left to right) 2D images: of the surface defects concentration structure formed at the cooperative nucleation stage at $T = 2000$, the initial relief structure at T_{growth}=0, and the final relief structure obtained as the solution of Eq. (14) with $\delta = 10^{-2}$ at T_{growth}=30 (black color corresponds to surface defect concentration and relief minima, white color corresponds to surface defect concentration and relief maxima); (bottom) corresponding 3D images

Fig.8 shows the cross section of the surface relief after more prolong growth

$(\boldsymbol{T_{growth} = 85})$.

Fig. 8. (Dashed curve) cross section of 3D image of initial surface relief obtained at the cooperative nucleation stage; (full curve) surface relief obtained by computer simulation of the KPZ equation (14) with $\delta = 10^{-2}$ at $T_{growth} = 85$

It is seen that the growth affects the depth of nanovoids and makes them less sharp.

1. Computer simulations of the DDKS and KPZ equations well above threshold of the DD surface instability. Formation of rough surface nanorelief structure at the nucleation stage

Now, we set in Eq.(5) the control parameters values Γ = 0.158 and ε = 2.4, corresponding to the wide excitation band (Fig.1, the upper curve $\lambda(Q)$). Fig.9 shows 3D images of surface defect concentration field obtained in this case by computer simulation of the DDKS equation (5) at different times.

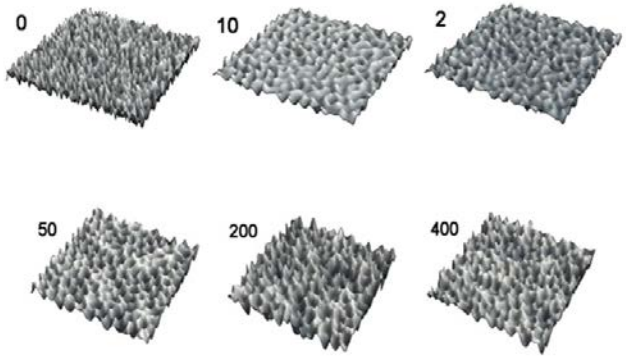

Fig. 9. 3D images of surface defect concentration field obtained by computer simulation of the DDKS equation (5) with Γ = 0.158 and ε = 2.4 formed at different nucleation times *T*=0, 2, 10, 50, 200 and 400

It is seen that at these values of control parameters, the disordered seeding structure of surface defect concentration is formed. Fig.10 shows corresponding images of 3D Fourier-spectrum elucidating the dynamics of formation of this structure.

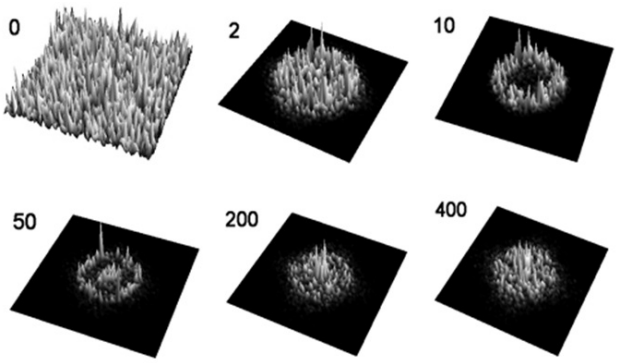

Fig. 10. Images of 3D Fourier-spectrum of the surface defect concentration field corresponding to Fig.10

It is seen that, in case of initially wide excitation band (Fig.1, the upper curve $\lambda(Q)$), the generation of difference of wavevectors ending on the thick ring, formed on the linear stage of the DD instability (nucleation time *T*=10), leads to the appearance of low spatial frequency DD harmonics (*T*=50), so that eventually the whole area within the ring become excited (*T*=400).

To show how this Fourier-spectrum transformation affect the morphology of the surface, we transform the final image of defect concentration field (Fig.11, nucleation time *T*=400) using Eq.(12), where $\theta_d < 0$, to the seeding surface relief structure (Fig.11, *T*=0) and the latter was used as the initial condition for simulation of nanoparticle ensemble growth with the help of KPZ equation (14). The resulting disordered, rough surface relief is shown in Fig. 11, *T*=10.

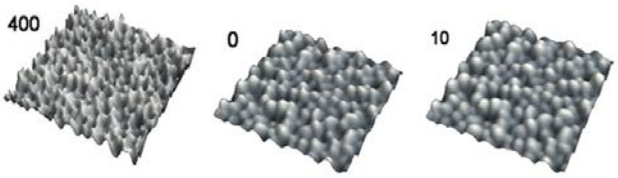

Fig.11. The 3D image of the final surface defect concentration field formed in the cooperative DD nucleation (nucleation time *T* = 400), the initial (prior to the growth) surface relief in the case (*T*growth=0) and the final surface relief obtained by computer simulation of KPZ Eq. (14) with $\delta = 10^{-2}$ (*T*growth=10)

4. Comparison with experimental data

4.1. Comparison of the theory and experimental results on void nanostructure formation

Authors of [15] have reported the self-organized growth of ordered structures of voids with the hexagonal symmetry on a Pt-modified Ge(001) (Pt/Ge-(001)) surface. Initially a frac-

tion of a Pt monolayer was deposited on a clean Ge(001) surface (with an area of 80×80 nm^2), then the sample was annealed several times at a temperature 1100 (±50) K, subsequently a 0.2 – 0.5 monolayer of Pt was deposited on the substrate, and after prolonged annealing at 1050 (±25) K was cooled to a temperature 77 K to provide STM measurements. A new well-ordered and densely packed phase of arrays of voids with a very narrow size distribution was found.

Fig. 12 shows comparison of the nanostructure of voids obtained by computer simulation with the experimental STM image obtained in [15]. Authors did not put forward a model explaining the formation of the ordered nanovoid domains, whereas the two-staged mechanism developed in the present paper is able to describe the formation of these ordered domains of nanovoids.

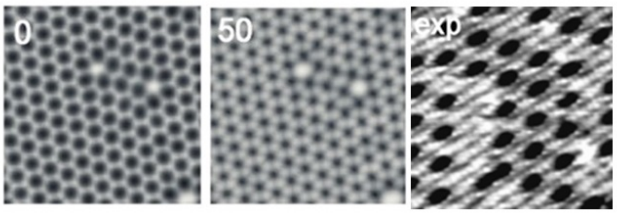

Fig. 12. (Top, from left to right) 2D images: of the initial (prior to the growth) surface relief in the case $\theta_d < 0$ (*T*growth=0), the final relief structure obtained by computer simulation of KPZ Eq. (14) with $\delta = 10^{-2}$ (*T*growth=50) and (exp) the experimental surface relief honeycomb structure (area: 13×13 nm2 [15]). Black color corresponds to surface relief minima, white color corresponds to surface relief maxima

4.2. Comparison of the theory and experimental results on nanoparticle ensemble formation

Authors of [16] studied the effect of laser excitation of Si $(100) - (2 \times 1)$ substrace for the process of Ge growth on it. In one of the experiments 22 monolayers of Ge were deposited at 250 ℃ with an excitation *s*-polarized laser energy density kept at 37 ± 4 mJ/cm^2, and an ablation *p*-polarized laser energy density at 5 J/cm^2. To model a surface relief structure measured in the experiment we employ the two-stage mechanism with the negative surface defect deformational potential $\theta_d < 0$.

The left-hand side of Fig.13 shows the comparison of the surface relief morphology obtained in [16] with the results of computer simulations of DDKS Eq.(5) and KPZ Eq.(14), wherein the control parameters have been chosen for the best similarity between them. On the right-hand side of Fig.13 the corresponding nanoparticle size distributions in ensembles are shown.

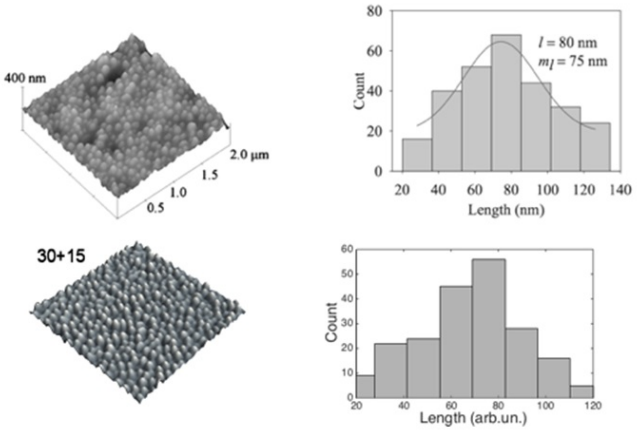

Fig. 13. (Top, from left to right): AFM image of the surface showing ensemble of Ge nanoparticles and nanoparticle size histogram from the AFM image [16]; (bottom, from left to right): 3D image of surface relief obtained by computer simulation of the KPZ Eq. (14) with $\delta = 10^{-2}$ at $T_{growth} = 15$, where the initial surface relief ($T_{growth} = 0$) is taken from computer simulation of the DDKS Eq. (5) at nucleation time $T = 30$ with $\Gamma = 0.158$, $\varepsilon = 2.18$ and the initial value of the defect concentration field given by white noise from the interval $[-2.5; 2.5]$, corresponding size histogram obtained from computer simulation.

One can see from Fig.13 that the simulation closely reproduces experimental results of Ref.[16].

5. Second harmonic and spatial sum-frequency generation

5.1. DD second harmonic and spatial sum-frequency generation

Formation of a stationary monodisperse honeycomb structure (superlattice) of surface defect concentration at the cooperative nucleation stage (Fig. 14a) is accompanied by the generation of DD second and sum-frequency harmonics owing to the nonlinearity of DDKS Eq. (5). It is seen from Fig. 14d which shows the Fourier-spectrum of superlattice with presence of second and sum-frequency harmonics as the result of DDKS Eq. (5) computer simulation ($T_{nucl} = 2000$).

Let's transform DDKS Eq.(5) into Fourier space to describe nonlinear interactions of spatial DD harmonics (below, we designate the dimensionless wave vector $\mathbf{Q}$=*k*):

$$\frac{\partial n(\mathbf{k})}{\partial t} = [-\Gamma + \mathbf{k}^2(\varepsilon - 1) - \varepsilon\mathbf{k}^4]n(\mathbf{k}) + \\ + \sum_{\mathbf{k}'} \mathbf{k}' \cdot (\mathbf{k} - \mathbf{k}')n(\mathbf{k}')n(\mathbf{k} - \mathbf{k}') \qquad (15)$$

The linear part of the Eq.(15) leads to the formation of a ring of harmonics at a linear stage of temporal evolution. Then, the nonlinear part of the Eq.(15) gives rise to the angular selection of fundamental modes, corresponding to three fundamental DD gratings. The nonlinear interaction of fundamental harmonics leads to extra reflexes formation in Fig. 14d-f. For example, the mechanism of the spatial second harmonic $\mathbf{2k_1}$ generation (Fig.14f) is described by the interaction of the two fundamental harmonics $\mathbf{k_1}$ via the nonlinear term:

$$\frac{\partial n(\mathbf{2k_1})}{\partial t} = [-\Gamma + (\mathbf{2k_1})^2(\varepsilon - 1) - \\ -\varepsilon(\mathbf{2k_1})^4]n(\mathbf{2k_1}) + \left(\mathbf{k_1}n(\mathbf{k_1})\right)^2. \qquad (16)$$

The process of the harmonic summation $(\mathbf{k_1} + \mathbf{k_2})$ (Fig.14f) is described by the interaction of two fundamental modes $\mathbf{k_1}$ and $\mathbf{k_2}$:

$$\frac{\partial n(\mathbf{k_1}+\mathbf{k_2})}{\partial t} = [-\Gamma + (\mathbf{k_1} + \mathbf{k_2})^2(\varepsilon - 1) - \\ -\varepsilon(\mathbf{k_1} + \mathbf{k_2})^4]n(\mathbf{k_1} + \mathbf{k_2}) + \\ +(\mathbf{k_1}+\mathbf{k_2})n(\mathbf{k_1})n(\mathbf{k_2}). \qquad (17)$$

Also, Fig. 14a demonstrates the presence of superlattice localized defects which give rise to the enrichment of the spectrum (Fig. 14d). In Fig. 14d reflexes of fundamental, second and spatial sum-frequency harmonics are surrounded by additional noise reflexes, associated with superlattice defects. We will discuss the relation of superlattice defects (Fig. 14a) to this additional noise spectrum (Fig. 14d) in Sec. 5.2. We suggest also a method to eliminate these superlattice defects and damp out corresponding DD harmonics.

5.2. Purification of modeled supercrystalline structure using the stochastic DDKS equation

In Fig.14d, corresponding to nucleation stage, besides fundamental and second harmonic reflexes, also a parasitic noise spectrum occurring due to superlattice defects (Fig. 14a) is clearly seen, which distorts contribution of the DD second and sum harmonics. To damp out this parasitic noise spectrum (i.e. to eliminate superdefects) , we suggest to use the stochastic version of the DDKS equation, which can be written as

$$\frac{\partial n}{\partial T} = -\Gamma n - (\varepsilon - 1)\Delta n - \varepsilon\Delta^2 n - (\nabla n)^2 + f\,, \qquad (18)$$

where $f = f(\mathbf{R}, T)$ is a Gaussian noise source with neither space nor time correlation, zero mean and a relatively small dispersion σ^2 ($\sigma \ll \varepsilon$). The noise emergence could be caused by the inhomogeneity of the rate of adatom generation, whilst in the original DDKS Eq.(5) this rate is supposed to be constant and spatially uniform. We call it the stochastic purification stage, because it leads to elimination of superlattice defects (Fig.14a,b) and to the formation of regular hexagonal supercrystalline structure (Fig.14c).

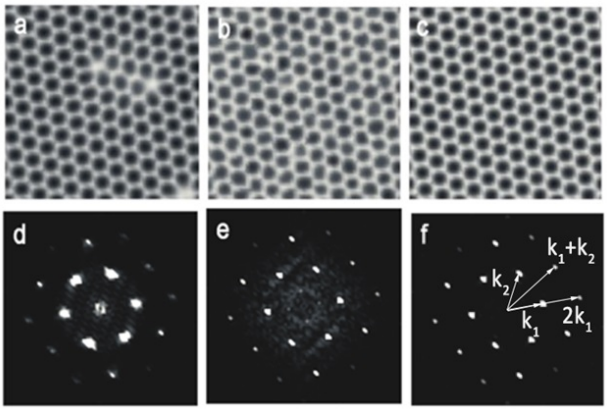

Fig. 14. 2D images: of the adatom concentration structure formed (a) at the cooperative nucleation stage at time $T = 2000$ (computer simulation of the DDKS Eq. (5)); (b) at the stochastic purification stage ($T_{pur} = 2000$, computer simulation of the stochastic DDKS equation (18)), (c) at the continuation of the cooperative nucleation stage at $T_{nucl} = 300$ of computer simulation of the DDKS equation (5); (d), (e) and (f) are images of 2D Fourier-spectrum corresponding to the images of the surface defect concentration (a), (b), (c)

Figs.14d-f shows the purification process of Fourier-spectrum of the adatom concentration or, in other words, the selection of fundamental, second and spatial sum frequency harmonics in the spectrum (Fig.14f).

The results obtained above suggest a method of supercrystalline structure purification by the addition of an extra spatially non-uniform noise to atomic deposition rate.

5.3. The establishment of the steady-state due to the second and sum-frequency harmonics generation

From Fig. 14 it is seen that the fundamental, the second and the sum frequency harmonics reflexes coexist and remain unchanged even at long times (the steady state). Let us discuss the mechanism of establishing of the steady state due to nonlinear interactions of DD harmonics.

At the linear stage of the surface DD instability, the exponential independent growth of Fourier amplitudes of a ring of fundamental harmonics lying within the excitation band (Fig.1) and decay of other harmonics occur, that leads to a non-stationary evolution of the solution. The amplitude of the fundamental superlattice grows, the relative role of nonlinear effects increases, then a selection of three fundamental modes occurs. The subsequent amplification of these fundamental harmonics leads to the efficient nonlinear interaction between them, due to the nonlinear term in Eq.(15), leading to the generation of second and sum-frequency harmonics described by Eq.(16) and Eq.(17). Eventually, the effect of exponential growth of fundamental harmonics is balanced by the nonlinear generation of second and sum-frequency harmonics, which also decay exponentially, because they lie in the stable region, outside the excitation band (Fig.1). Due to above interactions, the steady state is established (steady-state solution of Eq.(15)). Thus, the steady-state is reached due to nonlinear transformation of fundamental modes to second and sum-frequency harmonics balanced by their linear decay.

Therefore, the role of DD second and sum-frequency harmonics generation for the existence of stationary solutions of Eq.(5) is crucial. To check this, we have simulated damping out of these harmonics (Fig.15, $T = 0$), which gives rise to a new cycle of nucleation, when the angular symmetry is broken (Fig.15, $T = 30$) and a new ring of harmonics is generated (Fig.15, $T = 100$) as at the initial linear stage of nucleation from a spatial white noise seed.

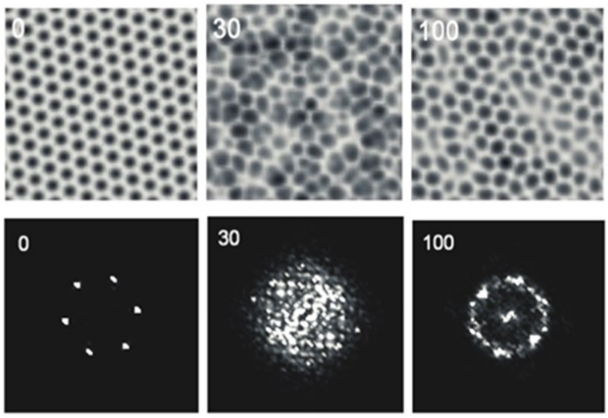

Fig. 15. (Top, from left to right) 2D images: of the surface defects concentration structure formed after damping out of the second and sum harmonics at $T_{nucl} = 0, 30, 100$ of computer simulation of the DDKS Eq. (5), (bottom, from left to right) images of 2D Fourier-spectrum corresponding to the images of the surface defect concentration

Although the amplitude of second and sum harmonics are an order of magnitude smaller than the amplitude of fundamental harmonics, their contribution to the resulting stationary solution is nevertheless crucial. The elimination of these harmonics leads to the elimination of a drain of fundamental Fourier amplitudes of adatom concentration in the model described above, that gives rise to a new cycle of cooperative nucleation and to the re-establishment of the necessary drain.

3. The parametric decay of the fundamental DD harmonic

In Fig.17 (at $T = 2000$) the parametric decay takes place, where a mode $\mathbf{k}$ decays into two modes $\mathbf{k_1}, \mathbf{k_2}$ and phase matching condition $\mathbf{k} = \mathbf{k_1} + \mathbf{k_2}$ is satisfied. In that case, the parametric decay during cooperative nucleation stage is described by the following set of coupled equations:

$$\frac{\partial n(\mathbf{k_1})}{\partial t} = [-\Gamma + (\mathbf{k_1})^2(\varepsilon - 1) - \varepsilon(\mathbf{k_1}/\mathbf{2})^4]n(\mathbf{k_1}) - \\ -(\mathbf{k}\cdot\mathbf{k_2})n(\mathbf{k})n(-\mathbf{k_2}) + \quad (19)$$

$$\frac{\partial n(\mathbf{k_2})}{\partial t} = [-\Gamma + (\mathbf{k_2})^2(\varepsilon - 1) - \varepsilon(\mathbf{k_2})^4]n(\mathbf{k_2}) - \\ -(\mathbf{k}\cdot\mathbf{k_1})n(\mathbf{k})n(-\mathbf{k_1}) + \quad (20)$$

where the terms responsible for the parametric decay are taken out of the sums.

To investigate numerically a process of DD parametric decay we employ the same control parameter values Γ = 0.158 and ε = 2.4 as in Figs. 9-11, corresponding to the wide excitation band $\lambda(Q)$(Fig.1) , however a computational time and a spatial grid size were increased to approach a highly nonlinear regime of the adatom concentration dynamics more accurately.

As a result we have found, that in the highly nonlinear regime, a bimodal ensemble with latent hexagonal symmetry is formed (Fig. 16).

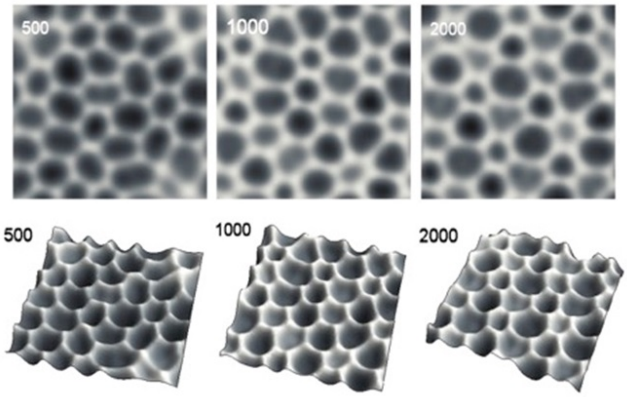

Fig. 16. (Top, from left to right) 2D images: of the surface defects concentration structure formed at the cooperative nucleation stage at nucleation time T = , $T = 1000$ and $T = 2000$ obtained by computer simulation of the DDKS Eq. (5) with Γ = 0.158 and ε = 2.4 (black color corresponds to surface defect concentration minima, white color corresponds to concentration maxima); (bottom) corresponding 3D images.

A Fourier-spectrum on Fig. 17 shows the effect of the nonlinear DD harmonics interaction: the parametric decay of the DD fundamental harmonics: $\mathbf{k} = \mathbf{k_1} + \mathbf{k_2}$.

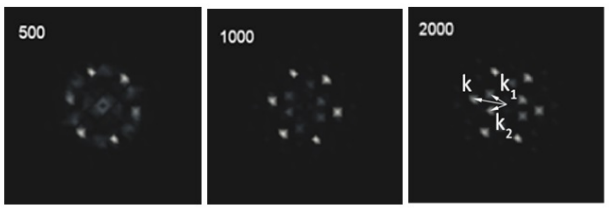

Fig. 17. (From left to right) Images of 2D Fourier-spectrum of the adatom concentration field corresponding to the cooperative nucleation stage at $T = 500$, $T = 1000$ and $T = 2000$.

The growth stage (Fig. 18) does not significantly affect the structural properties of nanoparticles, but leads to the closer packing of the bimodal ensemble particles and to the shape deformation of these particles. Therefore the structural properties of emerging nanoparticle and nanovoid ensembles are formed at the nucleation stage, while the growth stage changes individual geometrical characteristics of nanoparticles.

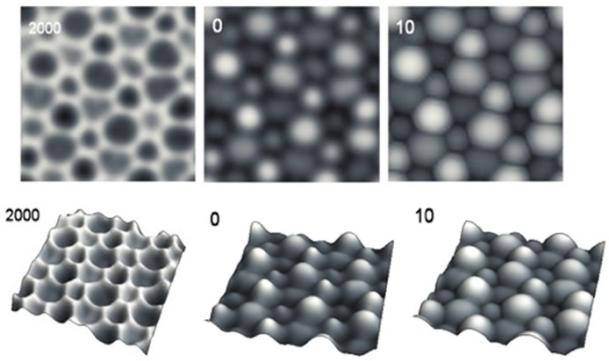

Fig. 18. (Top, from left to right) 2D images: of the surface defects concentration structure formed at the cooperative nucleation stage at T_{nucl}=2000, the initial relief structure T_{gr}=0, and the final relief structure obtained as the solution of Eq. (25) with $\delta = 10^{-2}$ at T_{growth}=10 (black color corresponds to the surface relief and defect concentration minima, white color corresponds to the surface relief and defect concentration maxima); (bottom) corresponding 3D images.

From the phase matching condition $\mathbf{k} = \mathbf{k_1} + \mathbf{k_2}$ we can derive $|\mathbf{k}| = \sqrt{3}|\mathbf{k_1}|$, and corresponding sizes of particles in a bimodal ensemble should satisfy the same condition $R = \sqrt{3}r$, where R and r are the radii of big and small particles respectively.

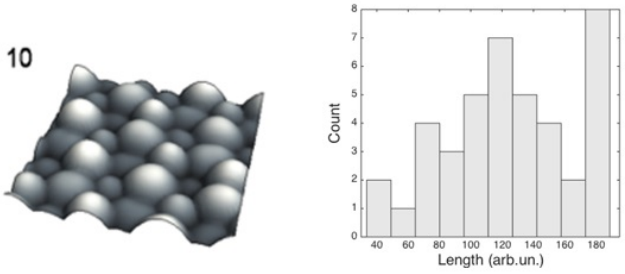

Fig. 19. (From left to right) 3D image of the final relief structure from Fig.18 ($T = 10$), the bimodal nanoparticle size histogram corresponding to this relief

In Fig.19, the corresponding nanoparticle size histogram is shown which has two maxima with a size ratio of 0.6, which is in a good agreement with $1/\sqrt{3}$ obtained from the phase matching condition. Bimodal ensembles with a similar size ratio were obtained in an experiment of deposition of Ge nanoparticles on the Si substrate in a presence of laser radiation [20].

Conclusion

In conclusion, the two-stage mechanism of the DD cooperative nucleation and subsequent growth of nanostructures on the surface with mobile adatoms (surface defects) is developed. At the first, cooperative nucleation stage, described by the original DDKS equation [11], the universal honeycomb void structure of surface defects is formed which serves as a seeding structure for the subsequent growth. This is explained by the fact that the DDKS equation for surface defect concentration involves the gradient quadratic term with negative sign.

The growth stage is described by the conventional KPZ equation. The type of final nanostructure of surface relief, formed at the second, growth stage depends on the sign of surface defect deformation potential θ_d. In case of positive deformation potential, the final honeycomb void nanostructure is formed, while in case of negative deformation potential, the hexagonal ensemble of nanoparticles (mounds) is formed. In this respect, the two-stage mechanism, described by both nucleation DDKS and growth KPZ equations is more flexible than one-stage growth mechanism. In contradistinction to the DDKS equation [11], the KS equations for the surface relief corrugation *h*, describing surface nanostructuring in ion sputtering [17,18] or in laser ablation[6,19] have quadratic nonlinearity with positive sign.

The symmetry and periodicity of final nanostructures is prescribed by corresponding characteristics of final nucleated void structure of surface defect concentration. The period of nanostructure (the characteristic size of voids or nanoparticles) is proportional to the length of nonlocal adatom-strain interaction l_d (scaling parameter of nonlocal elasticity theory [9]). Determination of l_d, as well as the calculation of θ_d, are important problems which can be addressed after specification of parameters of materials of interest and nature of surface defects.

Two externally controlled parameters determine the symmetry of the nucleated nanostructure: the spatially uniform (mean) surface defect concentration ε and surface defect relaxation constant Γ. As it was shown, the choice of control parameters determines the character of temporal evolution of the Fourier-spectrum governed by nonlinear DD harmonics interactions. This was demonstrated in two cases of small and large exceeding over the DD surface instability threshold. The practical recommendation following from this consideration is to achieve formation of hexagonally ordered surface structure of nanovoids or nanoparticles it is necessary to carry out the deposition just above threshold. The determination of the full phase diagram, displaying regions of control parameters ε and Γ corresponding to formation of different types of nanostructures needs more extensive studies of the DDKS equation.

In the highly nonlinear regime, higher order DD harmonics generation was found. In the case of small exceeding over the DD surface instability threshold, the spatial second harmonic generation and sum-frequency generation take place, which was found to be crucial for the existence of stationary solutions of DDKS equation. The method of stochastic purification of supercrystalline structure from superlattice defects is suggested. In case of large exceeding over the threshold, parametric DD decay and sum-frequency generation are observed, consequently leading to the formation of a bimodal particle ensemble.

The relevance of the developed two-stage mechanism to experimental data was shown on the examples of the honeycomb void structure and hexagonal particle ensemble formation under positive atomic (arrival of atoms on the surface). The morphology of the numerically obtained structures is similar to experimental ones.

We suppose that the developed here for the case of positive atomic deposition two-stage mechanism of nanostructure formation can be used also in the case of surface nanostructuring under negative atomic deposition (removal of atoms from the surface), for example, under ion sputtering or laser ablation.

Список литературы:

1. V. A. Shchukin and D. Bimberg, Rev. Mod. Phys. 71, 1125 (1999).
2. Y. Kuramoto, Chemical Oscillations, Waves and Turbulence (Springer, Berlin, 1984).
3. G. I. Sivashinsky, Ann. Rev. Fluid Mech. 15, 179 (1983).
4. J. M.Garcia, L. Vazquez, R. Cuerno, J. A. Garcia, M. Castro, R. Gago, "Towards Functional Nanomaterials," in Lecture Notes on Nanoscale Science and Technology, Ed. by Z. Wang (Springer, Heidelberg, 2009).
5. A.G. Limonov, Mathematical Models and Computer Simulations, 3, N2, 149 (2011).
6. J. Reif, O. Varlamova, S. Varlamov, M. Bestehorn, Appl. Phys. A, 104, 969 (2011).
7. V.I. Emel'yanov, Laser Physics, 2009, Vol. 19, No. 3, pp. 538–543.
8. V.I. Emel'yanov, in Laser ablation in liquids, Principles and applications in the preparation of nanomaterials, edited by G. Yang (Pan Stanford Publ., Singapore, 2012), Chap. 1, pp. 1–109.
9. V. I. Emel'yanov, A. I. Mikaberidze, Phys. Rev. B72, 235407 (2005).
10. V.I. Emel'yanov, A.S. Kuratov, Eur. Phys. J. B86, 270 (2013).
11. V.I. Emel'yanov, A.S, Kuratov, Eur. Phys. J. B86, 381 (2013).
12. M. Kardar, G. Parisi, Y.C. Zhang, Phys. Rev. Lett. 56, 889 (1986).
13. A.B. Al'shin, E.A. Al'shina, A.G. Limonov, Comput. Math. Math. Phys. 49, 261 (2009).
14. S.M. Cox, P.C. Matthews, J. of Comput. Phys., 176, 430 (2002).
15. A. Kumar, B. Poelsema, H.J. Zandvliet, J. Phys. Chem. C 115, 6726 (2011).
16. A.O. Er, H.E. Elsayed-Ali, J. of Appl. Phys. 108, 034303 (2010).
17. S. Facsko, T. Bobek, A. Stahl, H. Kurz, T. Dekorsky, Phys. Rev. B69, 153412 (2004).
18. T.C. Kim, C.M. Ghim, H.J. Kim, D.H. Kim, D.Y. Noh, N.D. Kim, J.W. Chung, J.S. Yang, Y.J. Chang, T.W. Noh, B. Kahng and J.-S. Kim, Phys. Rev. Lett. 92, 246104 (2004).
19. V.I. Emel'yanov, Laser Physics, 2011, Vol. 21, No. 1, pp. 222–228.
20. M.S. Hegazy, H.E. Elsayed-Ali, J. Appl. Phys. 104, 124302 (2008).–